

## Photocatalytic Activity of 2D Copper Porphyrin Metal-Organic Framework for Visible Light Overall Water

Andres Uscategui, Horatiu Szalad, Josep Albero and Hermenegildo Garcia

Instituto Universitario de Tecnología Química, Consejo Superior de Investigaciones Científicas-Universitat Politecnica de Valencia, Universitat Politecnica de Valencia, Av. De los Naranjos s/n, 46022 Valencia, Spain

### Experimental section

**2D Cu<sub>2</sub>(CuTCPP) synthesis:** 185 mg of Cu(NO<sub>3</sub>)<sub>2</sub>·3H<sub>2</sub>O (Merck) and 200 mg of the metal-free porphyrin (H<sub>2</sub>TCPP; Frontier Specialty Chemical) were dissolved together in 450 ml of DMF in a 500 mL round flask. Then, the obtained solution was sonicated for 10 minutes and, subsequently, the temperature of the solution was increased up to 85°C, and held for 24 h under vigorous stirring and reflux. The resulting purple solids were recovered by filtration and profusely washed with DMF and ethanol. Finally, the 2D MOF was further purified with methanol in a Soxhlet extractor and dried in vacuum at 150°C overnight.

### Characterization

PXRD patterns were acquired with a Shimadzu XRD-7000 diffractometer employing a Cu k<sub>α</sub> irradiation source (λ=1.5418 Å) operating at 40 kw and 40 mA. All data acquisition was done at a scanning speed of 10 °/min in the 2θ range 2-90 °. The chemical composition of all samples was determined via combustion chemical analysis employing a CHNS FISIONS elemental analyzer. DR UV-VIS spectra were acquired using a Varian Cary 5000 spectrophotometer in the range 200-800 nm. ATR-FTIR spectra were acquired with a Bruker Tensor 27 instrument equipped with a diamond ATR accessory. XPS analyses were recorded through a SPECS spectrometer equipped with a Phoibos 150 MCD-9 detector. The nonmonochromatic X-ray source composed of Al and Mg was operated at 200 W. Before data acquisition, the samples were evacuated at 10<sup>-9</sup> mbar in the spectrometer prechamber. The measured intensity ratios of the components were obtained from the area of the corresponding peaks after nonlinear Shirley-type background subtraction and corrected by the transition function of the spectrometer. FESEM images were acquired using a ZEISS GeminiSEM 500 electron microscope. The samples were applied directly on the support and subsequently investigated. TEM images were recorded via a JEOL JEM 2100F microscope operating under an accelerating voltage of 200 kV. The samples were uniformly dispersed in an

ethanol solution and subsequently dropped casted on carbon coated Ni TEM grids which were allowed to dry at room temperature. AFM measurements were carried out in a Bruker Multimode 8 Nanoscope instrument with a vertical resolution of 3 Å and a horizontal resolution of 5 nm

**Photocatalytic tests:** Photocatalytic H<sub>2</sub> evolution, O<sub>2</sub> evolution and overall water splitting were investigated upon irradiation of 1 mg/mL solutions containing the photocatalysts, water and the corresponding sacrificial agent (MeOH for H<sub>2</sub> evolution and Ce(NH<sub>4</sub>)<sub>2</sub>(NO<sub>3</sub>)<sub>6</sub> in the case of O<sub>2</sub> evolution), with a 150 W Xe Lamp (0.1 W/cm<sup>2</sup> intensity) filtered with a 450 nm cut-off filter. The reaction vessel is made of quartz and equipped with manometer. Prior photocatalytic reactions the suspensions were purged with Ar for 10 minutes and, eventually, the internal pressure assessed at 1 bar. Analysis of the evolved gases has been carried out through a micro-GC with two columns (Molsieve 5A and PorePlot Q) and TC detector that allowed us to monitor and quantify H<sub>2</sub>, O<sub>2</sub>, CO<sub>2</sub>, among other gases.

**Electrochemical characterization:** All photoelectrodes employed were prepared by drop-casting a dispersion of the CuTCPP MOF, ethanol and nafion binder onto FTO glass, which was subsequently left to dry at room temperature. All electrochemical experiments employed a one-compartment cell with a Ag/AgCl reference electrode and a platinum counter electrode. The electrolyte employed was a 0.1M aqueous solution of KCl. All photoelectrochemical data was acquired via a VersaStat3 potentiostation. The light source employed for the photoelectrochemical experiments was a 150 W Xe lamp equipped with an optical fibre, and the spectral contribution was adjusted via a 450 nm cut-off filter. Nyquist plot measurements were carried out both under light irradiation and dark conditions. Points were acquired in the frequency range of 0.1 – 10<sup>6</sup> Hz. Mott-Schottky experiments were preformatted under 5 different frequencies (1500, 1750, 2000, 2250 and 2500 Hz), and datapoints were acquired between -1 and 1V (vs Ag/AgCl). Photo-action data was recorded by irradiating the cell with a 150 W Xe lamp source light passing through a triple grating monochromator from Optics Focus. The light intensities were recorded via a photodiode system from Hamamatsu.

External quantum efficiency values (EQE) were calculated employing the following formulas:

$$SR(\lambda) = \frac{I(\lambda)}{P(\lambda)} \text{ in (A/W)}; \quad EQE(\lambda)\% = \frac{1240 \cdot SR(\lambda)}{\lambda} ;$$

where SR(λ) is the spectral response, I(λ) is the photocurrent recorded by the system upon light irradiation, P(λ) is the power of incident irradiation at each wavelength and λ is the wavelength of the incident photons.

**Table S1.** Analytical data of the samples under study obtained from combustion elemental analysis and ICP-OES.

	C (wt.%)	H (wt.%)	N (wt.%)	O (wt.%)	Cu (wt.%)	Fe (wt.%)
Cu <sub>2</sub> (CuTCPP)	57.9	2.8	6.4	16.9	16.0	-
Cu <sub>2</sub> (FeTCPP)	-	-	-	-	9.2	3.9

**Table S2.** Summary of some reported examples of MOF-based photocatalysts for overall water splitting including the light source conditions, productivity and stability.

Photocatalysts	Reaction conditions	Photocatalytic activity	Stability	Ref.
Al-ATA-Ni	300W Xe lamp	66.7 $\mu\text{L/h H}_2$ and 33.3 $\mu\text{L/h O}_2$		1
Pt@NH <sub>2</sub> -UiO-66@MnO <sub>x</sub>	300+UV arc lamp with a UV-cut off filter ( $\lambda \geq 400$ nm)	20 $\mu\text{mol/g}\cdot\text{h H}_2$ 10 $\mu\text{mol/g}\cdot\text{h O}_2$	-	2
IEF-13	UV-vis 150 W Xe lamp	160 $\mu\text{mol/g H}_2$ 46 $\mu\text{mol/g O}_2$	22h	3
Pt and RuO <sub>x</sub> , MIL-125(Ti)-NH <sub>2</sub>	300 W Xenon lamp	218 and 85 $\mu\text{mol/g}_{\text{photocatalyst}}$ at 24 h for H <sub>2</sub> and O <sub>2</sub> , respectively	24h	4
IEF-11	simulated sunlight	672 $\mu\text{mol/g}_{\text{catalyst}}$ in 22 h of H <sub>2</sub>	10 d	5
UiO-66(Zr/Ce/Ti)	xenon lamp (150 mW cm <sup>-2</sup> )	230 and 110 $\mu\text{mol/g}$ of H <sub>2</sub> and O <sub>2</sub> , respectively, upon UV light irradiation, and 210 and 70 $\mu\text{mol/g}$ of H <sub>2</sub> and O <sub>2</sub> , respectively, under visible light irradiation	24h	6
Liposome-MOF@Pt-porphyrin and Ir-bipyridine	400 nm + 450 nm LEDs	836 $\mu\text{mol g}^{-1}$ of H <sub>2</sub> and stoichiometric amounts of O <sub>2</sub>	72 h	7
MIL-125(Ti)-CoPi-Pt	Xe lamp (300 W) 1 mg/mL	42 $\mu\text{L/h H}_2$ and 21 $\mu\text{L/h O}_2$	-	8
Cu <sub>2</sub> (CuTCPP)	LED (visible light) ( $\lambda > 450$ nm)	120 $\mu\text{mol}_{\text{H}_2} \text{g}_{\text{catalyst}}^{-1} \text{h}^{-1}$	5 consecutive uses	This report

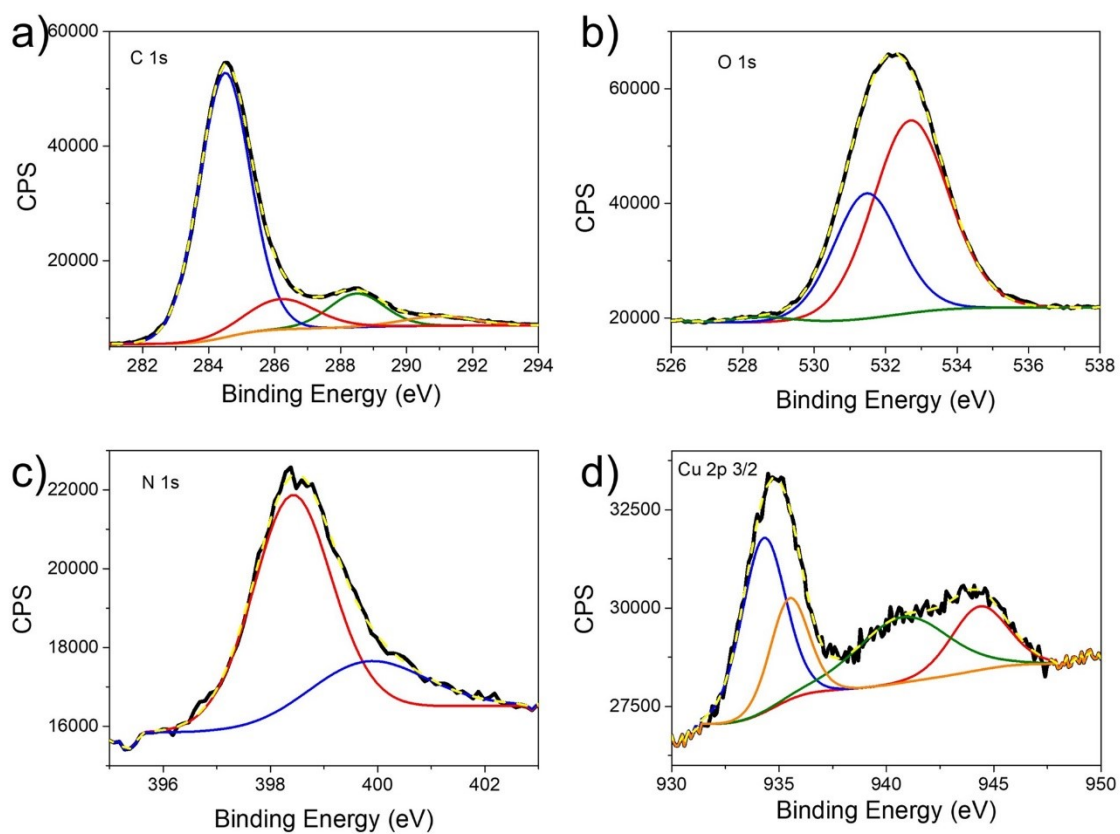


**Figure S1.** High-resolution XPS spectra and their best deconvolution of C1s (a), O 1s (b), N 1s(c) and Cu 2p 3/2 (d) of  $\text{Cu}_2(\text{CuTCPP})$ .

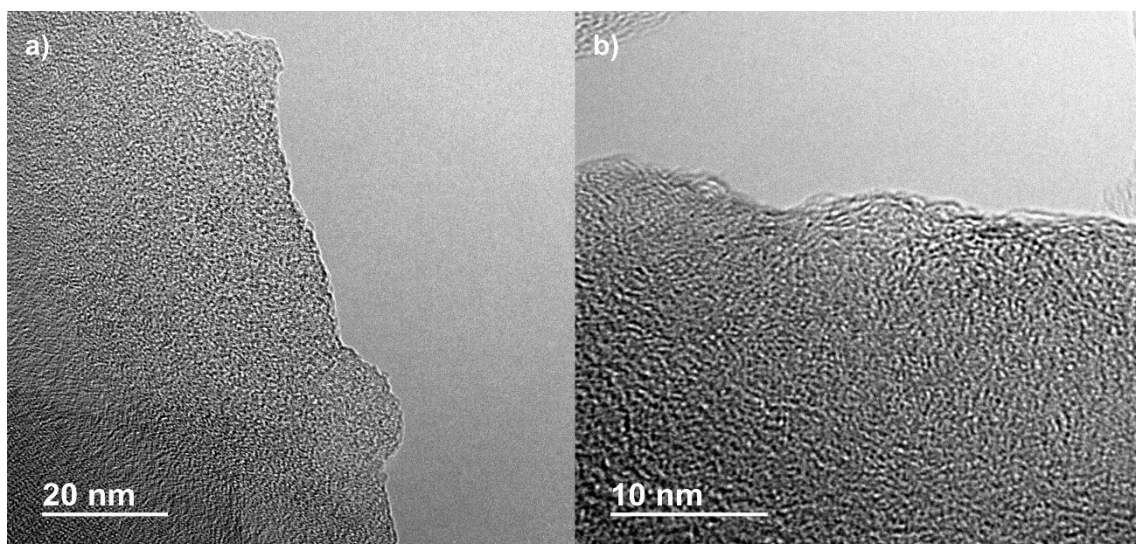


**Figure S2.** HRTEM images of the  $\text{Cu}_2(\text{CuTCPP})$  MOF.

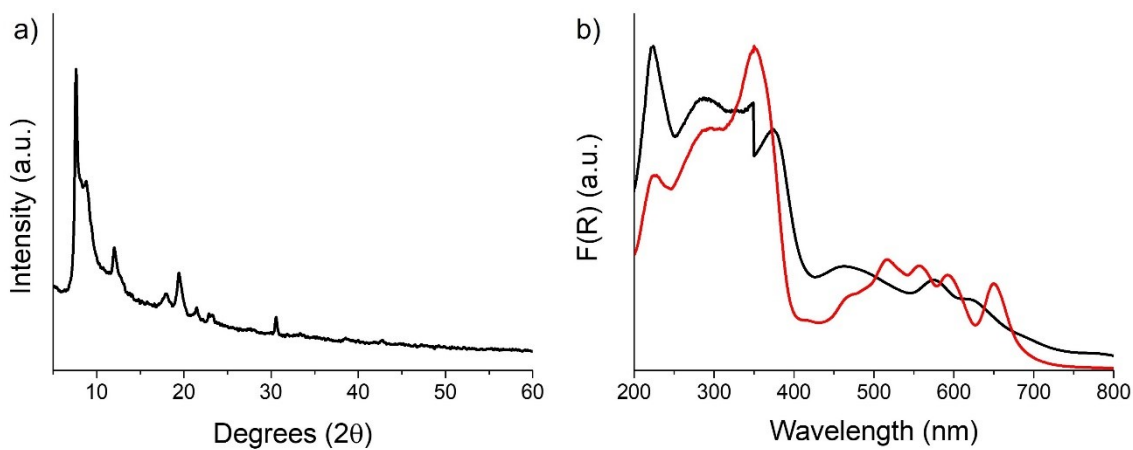


**Figure S3.** (a) XRD pattern of  $\text{Cu}_2(\text{FeTCPP})$  and (b) diffuse reflectance UV-vis spectra of  $\text{Cu}_2(\text{FeTCPP})$  (black) and  $\text{H}_2\text{TCPP}$  (red).

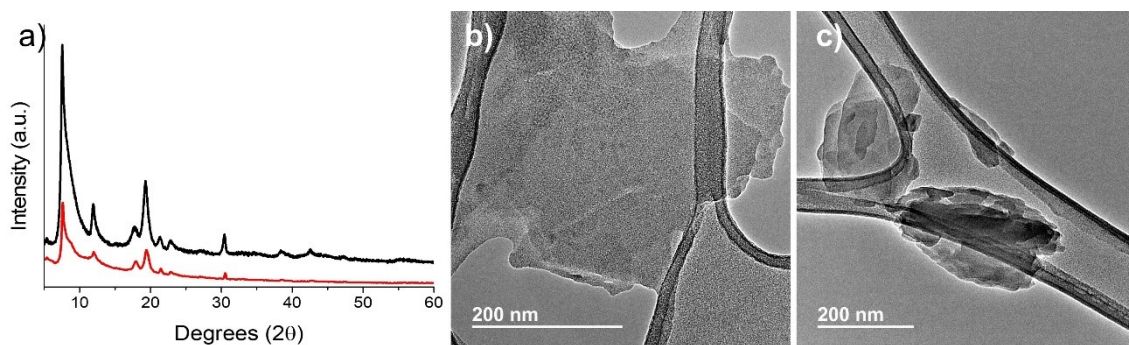


**Figure S4.** (a) XRD pattern of fresh (black) and after 5 uses (red)  $\text{Cu}_2(\text{CuTCPP})$ . (b) TEM image of as-prepared  $\text{Cu}_2(\text{CuTCPP})$ . (c) TEM image of  $\text{Cu}_2(\text{CuTCPP})$  after 5 uses.

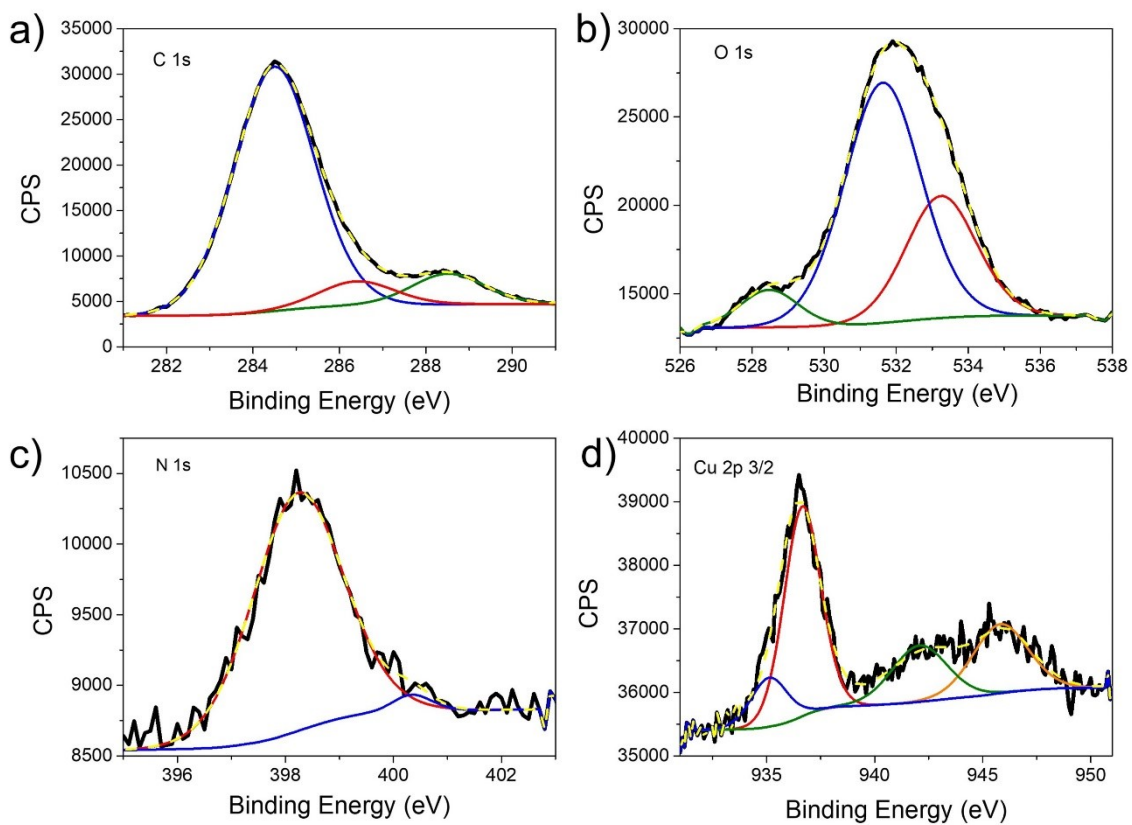


**Figure S5.** High-resolution XPS spectra and their best deconvolution of C1s (a), O 1s (b), N 1s(c) and Cu 2p 3/2 (d) of  $\text{Cu}_2(\text{CuTCPP})$  after 5 consecutive uses.

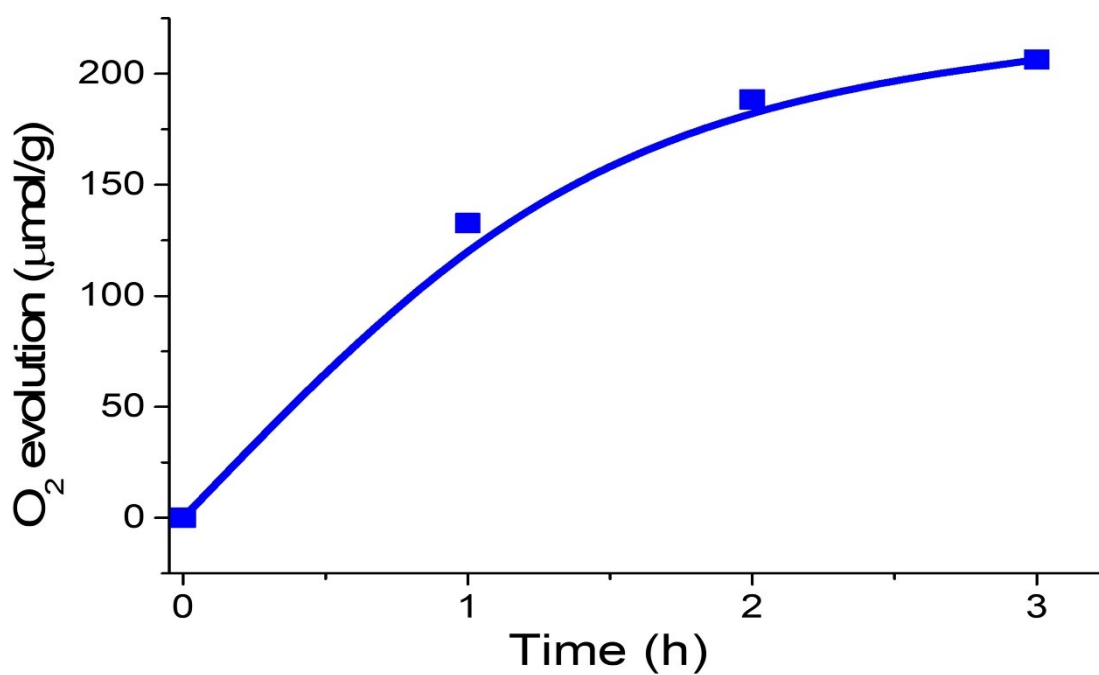


**Figure S6.** O<sub>2</sub> evolution under visible light irradiation ( $\lambda > 450$  nm) in the presence of Ce(NH<sub>4</sub>)<sub>2</sub>(NO<sub>3</sub>)<sub>6</sub> as sacrificial electron acceptor agent.

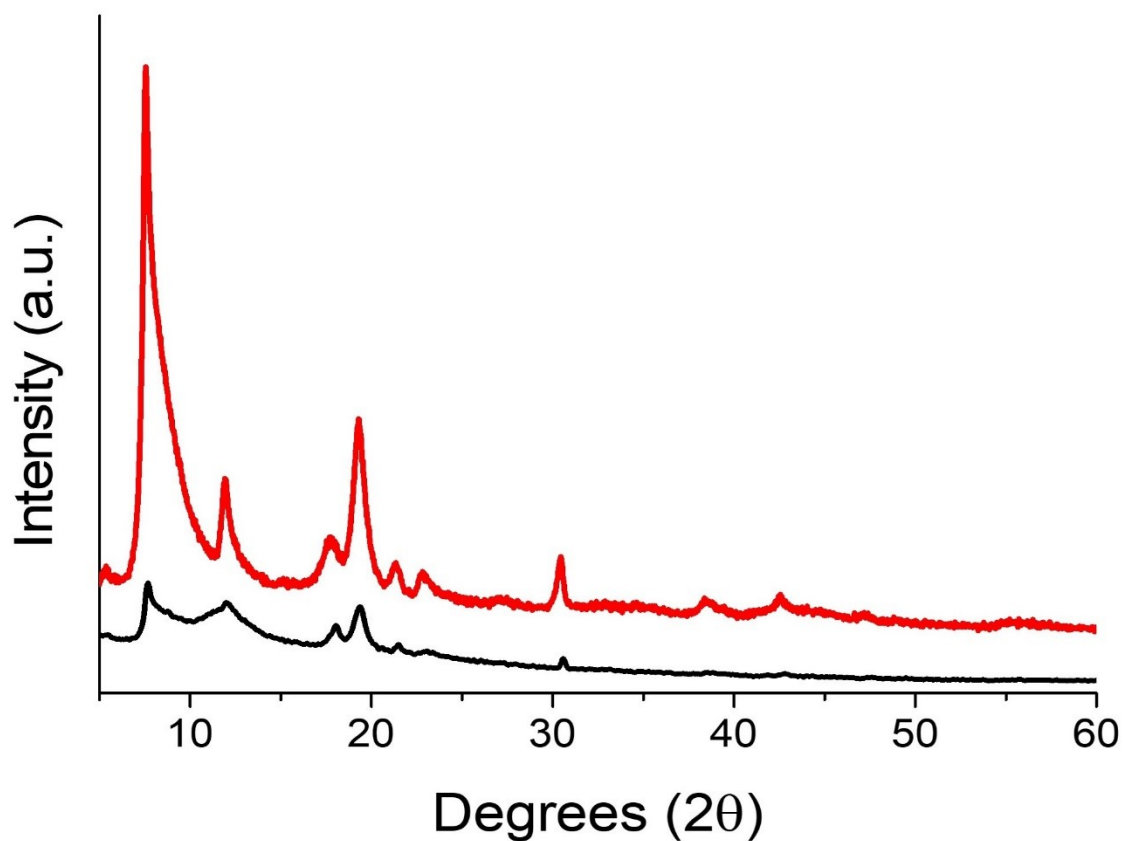


**Figure S7.** XRD pattern of Cu<sub>2</sub>(CuTCPP) prior (red) and after (black) photocatalytic overall water splitting reaction.

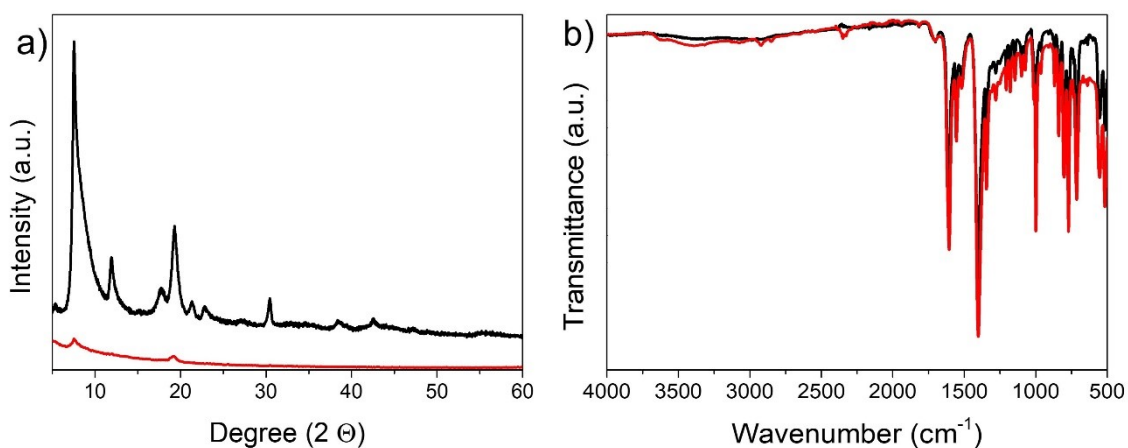


**Figure S8.** XRD patterns (a) and FTIR spectra (b) of Cu<sub>2</sub>(CuTCPP) prior (black) and UV irradiated (red).

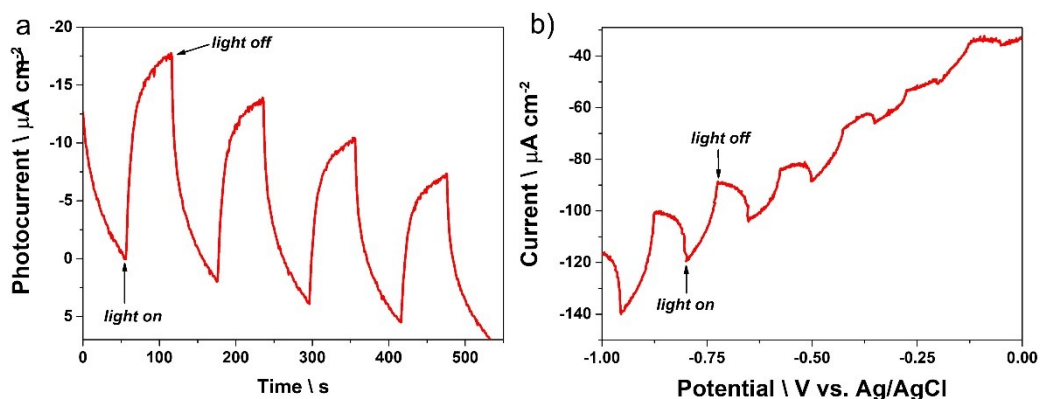


**Figure S9.** Photocurrent experiments in  $\text{Cu}_2(\text{CuTCPP})$ -based photoelectrodes at  $-0.28\text{ V}$  vs. NHE (a) and under voltage increase from 0 to  $-1\text{ V}$  vs. Ag/AgCl. Aqueous electrolyte at  $0.1\text{ M}$  KCl. Pt wire and Ag/AgCl as counter and reference electrodes, respectively. Electrolyte:  $0.1\text{M}$  aqueous solution of KCl.

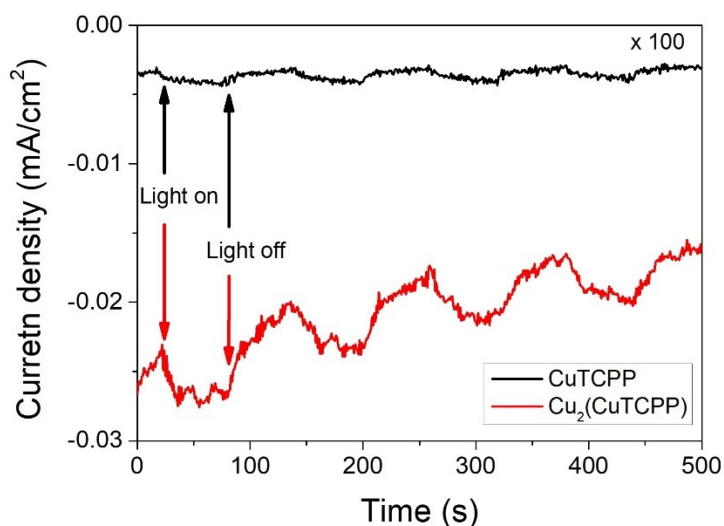


**Figure S10.** Photocurrent experiments in  $\text{Cu}_2(\text{CuTCPP})$  and CuTCPP-based photoelectrodes at  $-0.1\text{ V}$  vs. Ag/AgCl. Aqueous electrolyte at  $0.1\text{ M}$  KCl. Pt wire and Ag/AgCl as counter and reference electrodes, respectively. Electrolyte:  $0.1\text{M}$  aqueous solution of KCl.



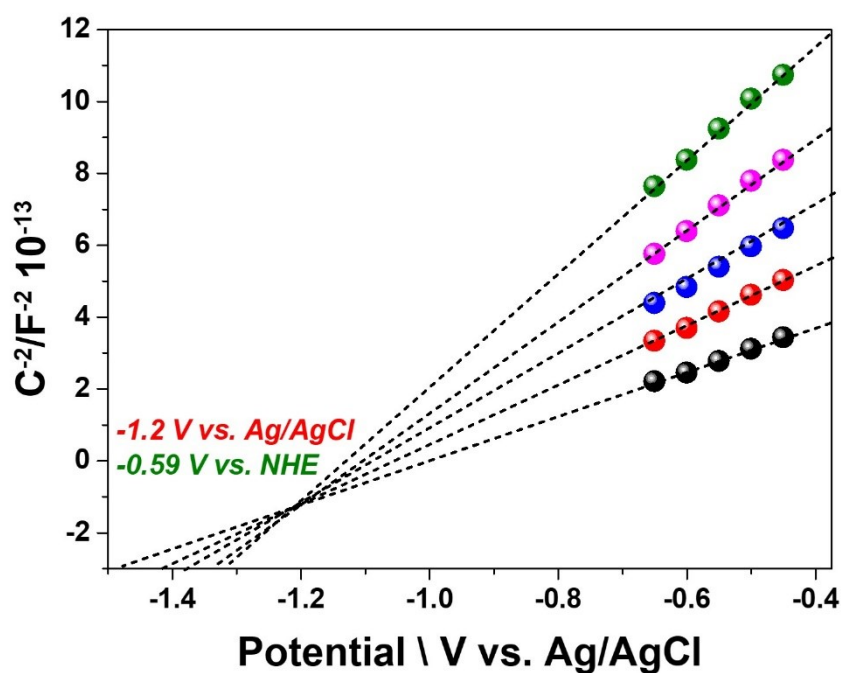


**Figure S11.** Mott-Schottky plot from a  $\text{Cu}_2(\text{CuTCPP})$ -based electrode, using a Pt wire and Ag/AgCl electrodes as counter and reference electrodes, respectively, and measured at 1500, 1750, 2000, 2250 and 2500 Hz frequencies. Electrolyte: 0.1M aqueous solution of KCl.

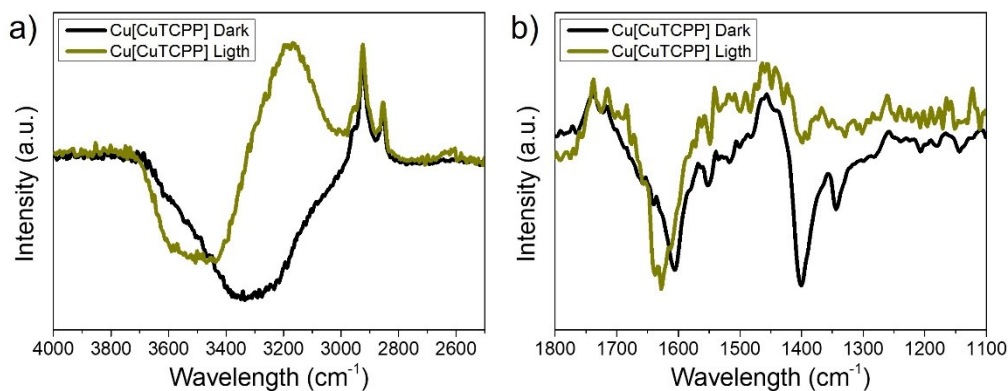


**Figure S12.** ATR-FTIR spectra of  $\text{Cu}_2(\text{CuTCPP})$  dispersion in ultrapure water in the dark (black) and under visible light irradiation (dark yellow) in the spectral regions from 2500 to 4000  $\text{cm}^{-1}$  (a) and from 1100 to 1800  $\text{cm}^{-1}$  (b). The aqueous  $\text{Cu}_2(\text{CuTCPP})$  dispersion spectra have been acquired after baseline subtraction. The baseline consisted in a ATR-FTIR measurement of a water drop.

## References

1. Y. An, Y. Liu, P. An, J. Dong, B. Xu, Y. Dai, X. Qin, X. Zhang, M.-H. Whangbo and B. Huang, 2017, **56**, 3036-3040.
2. J. Zhang, T. Bai, H. Huang, M.-H. Yu, X. Fan, Z. Chang and X.-H. Bu, 2020, **32**, 2004747.
3. P. Salcedo-Abraira, S. M. F. Vilela, A. A. Babaryk, M. Cabrero-Antonino, P. Gregorio, F. Salles, S. Navalón, H. García and P. Horcajada, *Nano Research*, 2021, **14**, 450-457.
4. S. Remiro-Buenamañana, M. Cabrero-Antonino, M. Martínez-Guanter, M. Álvaro, S. Navalón and H. García, *Applied Catalysis B: Environmental*, 2019, **254**, 677-684.
5. P. Salcedo-Abraira, A. A. Babaryk, E. Montero-Lanzuela, O. R. Contreras-Almengor, M. Cabrero-Antonino, E. S. Grape, T. Willhammar, S. Navalón, E. Elkäim, H. García and P. Horcajada, *Adv. Mater.*, 2021, **33**, 2106627.
6. A. Melillo, M. Cabrero-Antonino, S. Navalón, M. Álvaro, B. Ferrer and H. García, *Applied Catalysis B: Environmental*, 2020, **278**, 119345.
7. H. Hu, Z. Wang, L. Cao, L. Zeng, C. Zhang, W. Lin and C. Wang, *Nature Chemistry*, 2021, **13**, 358-366.
8. Y. An, B. Xu, Y. Liu, Z. Wang, P. Wang, Y. Dai, X. Qin, X. Zhang and B. Huang, 2017, **6**, 701-705.